



Cobalt and ruthenium complexes with pyrimidine based schiff base: Synthesis, characterization, anticancer activities and electrochemotherapy efficiency

Mehmet Eşref Alkış^a, Ünzile Keleştemür^a, Yusuf Alan^b, Nevin Turan^c, Kenan Buldurun^{d,*}

^a Department of Occupational Health and Safety, Faculty of Health Sciences, Muş Alparslan University, 49250 Muş, Turkey

^b Department of Primary Education, Education Faculty, Muş Alparslan University, 49250 Muş, Turkey

^c Department of Chemistry, Faculty of Arts and Sciences, Muş Alparslan University, 49250 Muş, Turkey

^d Department of Food Processing, Technical Sciences Vocational School, Muş Alparslan University, 49250 Muş, Turkey

ARTICLE INFO

Article history:

Received 5 September 2020

Revised 2 October 2020

Accepted 3 October 2020

Available online 5 October 2020

Keywords:

Schiff base

Metal complexes

Spectroscopy

Electrochemotherapy

Anticancer activity

ABSTRACT

In this study, a new Schiff base ligand and its two M(II) complexes [CoCl·L(H₂O)₂]-2H₂O, [RuCl(p-cymene)L] were synthesized. The structural features were confirmed from their micro analytical, IR, UV-Vis., ¹H-¹³C NMR, TGA, X-ray diffraction analysis, mass spectral data and magnetic susceptibility measurements. The Co(II) and Ru(II) complexes displayed an octahedral geometry. In vitro anticancer activities of the Schiff base, Co(II) and Ru(II) complexes were evaluated on the human colon cancer cell line (Caco-2) and biocompatibility characteristics were determined in the L-929 (normal fibroblast cells) cell line by using the MTT assay. Furthermore, we examined the effectiveness of electrochemotherapy (ECT) on cytotoxic activities of these compounds in Caco-2 cancer cell line. According to the findings of the study, Co(II) and Ru(II) complexes showed considerable anticancer properties in the Caco-2 colon cancer cells; however, the ligand did not show significant anticancer activity. It was determined that the combined application of electroporation (EP)+complexes were much more effective than the application of complexes alone in the treatment of Caco-2 colon cancer cells. In a conclusion, the Co(II) and Ru(II) complexes, which showed significant anticancer activity in Caco-2 colon cancer cells, increased cytotoxicity levels by 2.07 and 2.12, respectively in their combined applications with EP. These complexes can be developed as chemotherapeutic agents for colon cancer treatment and can yield promising results when used in ECT.

© 2020 Elsevier B.V. All rights reserved.

1. Introduction

Schiff bases constitute one of the most important classes of biologically active ligands due to their facile synthesis and good solubility [1]. They also connect with several transition metal atoms, forming important and stable complexes in many respects. Schiff bases containing donor atoms (e.g., N, O) play an important role in the transformation mechanism of some reactions in biological systems in neutral biological systems, especially thanks to the azomethine groups in their structure [2]. Their biological activities depend upon the type of substituent attached to the aromatic ring. Schiff bases have important biological activities such as antioxidant, antibacterial, antifungal, anticancer, and antidiabetic. Transition and non-transition metal complexes of azomethine moieties have biological and pharmacological properties, important in

catalysis, medicine, design of highly valuable materials, analytical chemistry as model compounds for structure and function of metalloproteins [3-7]. Cobalt complexes as potential anticancer agents have been the focus of interest for many researchers in the past decade. This effect was mainly attributed to its active role in the active center of vitamin B12, which regulates DNA synthesis. Also, cobalt is contained in the co-enzyme of vitamin B12, which is used as a vitamin supplement [8,9]. Ruthenium complexes are used as potential drug candidates in different biological studies, including anticancer, antimetastatic, antibacterial, and antifungal. Moreover, ruthenium complexes are interesting also as potential photochemotherapeutic anticancer agents [9-12].

Cancer continues to be a major threat for humans as the deadliest disease in the whole world. Colorectal cancer is the third most common cancer type among humans [13]. Treatment methods such as surgery, radiotherapy and chemotherapy are generally used in colon cancer. The anticancer drugs used in chemotherapy provide treatment with their effects on the life cycles of the cancer cells. These drugs are effective if they pass through the plasma

* Corresponding author.

E-mail address: k.buldurun@alparslan.edu.tr (K. Buldurun).

membrane, and achieve their intracellular targets like the DNA [14]. The resistance of the cell membrane against chemotherapy drugs is one of the most important factors preventing the success of cancer treatment [15]. Also, sometimes cancer cells can resist or develop resistance to these drugs [16]. For these reasons, although it is known that it has many side effects, long-term and high-dose anticancer drugs are used for effective treatment. Low effectiveness of medication in combination with a variety of side effects associated with chemotherapy causes a need to improve the therapeutic techniques and evaluation of new drugs. Today, Schiff bases and metal complexes with chemotherapeutic effects have become an area where medical chemists work intensively. In addition to the ligand effect, the choice of metal ion plays an important role in the target molecule to be selected, especially in the design of chemotherapeutic agents. These compounds show good selectivity against tumor cells, resulting in induction of apoptosis in cancer cells [17].

Electroporation (EP) is the process of increasing membrane permeability by applying electrical pulses to a biological cell or tissue for a short time and with a density that exceeds the capacitance of the cell membrane [18]. This method facilitates the entry of ions and molecules (weak or no permeant drug) into the cell, by creating temporary nanometer-sized small pores in the cell membrane [19]. In cancer treatment, the use of the agent combined with EP to increase the cytotoxic effect is called electrochemotherapy (ECT) [20]. Reversible EP (<1500 V/cm) can be used for the transfer of chemotherapeutic drugs to cells without damaging the cell viability [21]. Usually, square-wave electrical pulses with a duration of 100 μ s, at 1 Hz or 5 kHz frequency, 1000–1300 V/cm electrical field are used for ECT [18,22]. If the electrical field is applied when the extracellular concentration of the chemotherapeutic agent is at the highest level, the cytotoxicity may increase significantly by increasing the passage of the drug through the membrane. In this way, effective treatment will be achieved with a lower dose of the anticancer agents in a shorter time, and the side effects of chemotherapeutic agents are minimized [19]. Nowadays, ECT is mostly investigated for tumors located in the skin and deep under the skin, and for tumors in internal organs [23].

The design and development of new chemotherapeutic Schiff bases and metal complexes are now taking attention of medicinal chemists and works in this area is intensifying. Due to their interesting biological activities and our current concern [12,24], we synthesized and characterized the Schiff base ligand, Co(II) and Ru(II) complexes to obtain coordinated compounds with effective antitumor and anticancer activity. The anti-cancer activities of these compounds were investigated. We have investigated the relationship between co-ligand structure and the cytotoxicities of these complexes for human colon cancer cell lines as well as L929 normal cell lines. Furthermore, their ECT efficiency was evaluated.

A search through the literature reveals that no work has been done on the Co(II) and Ru(II) complexes and Schiff base formed by the condensation of 4-aminopyrimidine-2-(1H)-one with 2-hydroxy-3-methoxy benzaldehyde.

2. Experimental

2.1. General materials and methods

2-hydroxy-3-methoxy benzaldehyde, 4-aminopyrimidine-2-(1H)-one, $\text{CoCl}_2 \cdot 6\text{H}_2\text{O}$, $[\text{RuCl}_2(p\text{-cymene})]_2$, and ethanol, dimethyl sulfoxide (DMSO), acetone, dimethylformamide (DMF), chloroform, methanol, diethyl ether used in this study were purchased from Sigma-Aldrich and used without purification. Infrared spectra were performed by using Perkin Elmer FT-IR- 65 spectrometer (in the region 4000–400 cm^{-1} used by KBr pellets). ^1H (proton) and ^{13}C

(carbon) NMR spectra were mentioned on a Bruker 300 MHz spectrometer in DMSO-d_6 as the solvent. The microanalysis (C, H, N) were determined using a Vario III CHN analyzer. Mass spectra were performed with an Agilent technologies AB Sciex 3200 QTrap spectrometer. X-ray diffraction analysis was performed by an Ultima IV X-ray diffractometer with Rigaku ($\text{CuK}\alpha=1.540562 \text{ \AA}$). UV-Visible spectra were performed used through Shimadzu-UV-1800 spectrophotometer. Thermogravimetric analysis (TGA) was measured by an Universal TGA Q50 instrument at a heating rate of 10 $^\circ\text{C}/\text{min}$ between 50 and 900 $^\circ\text{C}$.

The L-929 and Caco-2 cell lines were used as models in our experiments. The Caco-2 cells (Passage No. 4) were provided from the Eastern Anatolia High Technology Application and Research Center (DAYTAM). The L-929 cell line (Passage No. 7) was obtained from the Biochemistry Department, Faculty of Science and Letters, Inönü University. The cells were seeded into 150 mL flasks by using Dulbecco's Modified Eagle's Medium (DMEM, Sigma) growth medium, to which 1% penicillin-streptomycin and 10% fetal bovine serum (Invitrogen, Carlsbad, CA) were added. The development of the cells was performed at 37 $^\circ\text{C}$ with 5% CO_2 and 95% humidity incubator (Esco, Singapore) medium. Biosafety Cabinet (ESCO, USA) was used for cell culture studies. ECT studies were performed in DAYTAM with Flow Cytometry (Becton-Dickinson) and Gene Pulsar Xcell™ (Bio-Rad, Hercules, CA, USA) devices.

2.2. Synthesis and characterization of ligand

(4-(2-hydroxy-3-methoxy benzylidene)amino)pyrimidine-2-(1H)-one (L)

4-aminopyrimidine-2-(1H)-one (1.0 mmol) was dissolved in methanol (20 mL). It was taken up with 2-hydroxy-3-methoxy benzaldehyde (1.0 mmol) dissolved in methanol (20 mL). The reaction mixture was refluxed for 5 h. The reaction result was determined by monitoring by TLC. Excess solvent was removed in the resulting rotary evaporator. The resulting product, washing several times with diethyl ether then was crystallized in methanol-chloroform (1/2 ration) mixture.

Ligand: Yield: 84%. m.p.: >260 $^\circ\text{C}$. Color: Dark white. Anal. Calcd. for $\text{C}_{12}\text{H}_{11}\text{N}_3\text{O}_3$ (FW: 245.23 g/mol) (%): C; 58.72, H; 4.52, N; 17.13. Found: C; 58.76, H; 4.55, N; 17.10. FT-IR (KBr, $\nu \text{ cm}^{-1}$): 3358 (OH), 3199 (NH), 3095 (Ar-CH), 2925 (Al-CH), 1716 (C = O), 1672 (CH=N), 1610 (CH=N pyrimidine), 1541, 1490, 1413 (C = C), 1230 (C-O), 1107 (OCH₃). ^1H NMR (300 Mz, DMSO-d_6): δ (ppm) = 11.40 (s, 1H, Ar-OH), 8.01 (s, 1H, NH), 8.85 (s, 1H, N=CH), 7.30–6.50 (m, 5H, Ar-H), 3.69 (s, 3H, OCH₃). ^{13}C NMR (75 Mz, DMSO-d_6): δ (ppm) = 159.70 (CH=N), 156.30 (C = O), 151.30 (C-OH), 149.10–110.50 (Ar-C), 54.30 (OCH₃). UV-Vis. (EtOH, λ_{max} , nm): 219, 247, 255, 261, 277, 283, 291, 297, 350, 360.

2.3. Synthesis and characterization of cobalt(II) and ruthenium(II) complexes

Schiff base (2.0 mmol) was dissolved in methanol (20 mL). $\text{CoCl}_2 \cdot 6\text{H}_2\text{O}$ (2.0 mmol) dissolved in methanol (10 mL) was added. The solution was refluxed for 4 h. The reaction was completed following the reaction by TLC. The precipitate formed was filtered, washed with diethyl ether, methanol and dried under vacuum. The methods of preparation for ruthenium (II) complex were similar to that of cobalt (II) complex except that $\text{CoCl}_2 \cdot 6\text{H}_2\text{O}$ was replaced with $[\text{RuCl}_2(p\text{-cymene})]_2$ (1.0 mmol).

$[\text{CoCl} \cdot \text{L}(\text{H}_2\text{O})_2] \cdot 2\text{H}_2\text{O}$: (FW: 410.38 g/mol) Anal. Calcd. for $(\text{C}_{12}\text{H}_{18}\text{N}_3\text{O}_7\text{CoCl})$: C; 35.08; H; 4.38, N; 10.23. Found: C; 35.10, H; 4.35, N; 10.27. FT-IR (KBr, $\nu \text{ cm}^{-1}$): 3425 (OH₂), 3172 (NH), 3077 (Ar-CH), 2998, 2929 (Al-CH), 1717 (C = O), 1658 (CH=N), 1605 (CH=N pyrimidine), 1537, 1513, 1465 (Ar-C = C), 1208 (C-O), 1106 (OCH₃), 857 (H₂O), 576, 544 (M-O), 506, 457 (M-N). UV-

Vis. (EtOH, λ_{\max} , nm): 224, 249, 274, 288, 295, 327, 386, 614, 648, 677. ESI-MS (m/z): 411.38 (Calcd.), 411.02 (Found) $[M + H]^+$. Color: Light blue.

[RuCl(*p*-cymene)L]: (FW: 514.87 g/mol) Anal. Calcd. for (C₂₂H₂₄N₃O₃RuCl): C; 51.27; H; 4.66, N; 8.15. Found: C; 51.35, H; 4.67, N; 8.20. FT-IR (KBr, ν cm⁻¹): 3115 (NH), 3095 (Ar-CH), 2918 (Al-CH), 1722 (C = O), 1653 (CH=N), 1609 (CH=N pyrimidine), 1573, 1541, 1490 (Ar-C = C), 1220 (C-O), 1106 (OCH₃), 885 (H₂O), 587, 532, 523 (M-O), 455 (M-N). ¹H NMR (300 Mz, CDCl₃): δ (ppm) = 8.10 (s, 1H, NH), 8.30 (s, 1H, N=CH), 7.22–6.90 (m, 9H, Ar-H), 3.73 (s, 3H, OCH₃), 1.24–1.18 (d, 6H, CH₃ of *p*-cymene), 2.32 (s, 3H, CH₃ of *p*-cymene), 2.86–2.83 (m, 1H, CH of *p*-cymene). ¹³C NMR (75 Mz, CDCl₃): δ (ppm) = 161.70 (CH=N), 157.23 (C = O), 151.70 (C-OH), 148.40–104.80 (Ar-C), 56.10 (OCH₃), 21.08 (CH₃ of *p*-cymene), 23.32 and 22.10 (CH₃ of *p*-cymene), 33.54 (CH of *p*-cymene). UV-Vis. (EtOH, λ_{\max} , nm): 221, 237, 247, 269, 286, 317, 350, 400. ESI-MS (m/z): 512.87 (Calcd.), 512.47 (Found) $[M-2H]^{-2}$. Color: Tile red.

2.4. In vitro anticancer activity

2.4.1. Chemotherapy

Cell counting device was used for counting the cells, and the viability rate was determined by using 0.4% trypan blue. All experiments were done when the viability rate was above 90%. Cell seeding was made to 96 wells plate as 1×10^4 cells in each well. The seeded cells were incubated for 24 h at 37 °C with 5% CO₂. After 24 h, the fluids were removed, 100 μ L of the 10; 25; 50; 100; 200; 300; 400; 500 and 600 μ M of the synthesized compounds solution prepared in the culture medium was added to each well, and was left for 24 h incubation again. The same concentrations were used in all MTT tests. Only 100 μ L culture medium (DMEM) was added to the cells in the control wells [25–27].

2.4.2. Determination of appropriate electrochemotherapy parameters

The purpose of trying to find the optimum ECT parameters was to determine the voltage values with sufficient power and time to provide the best permeability without too much damaging the cell viability [28]. When the Caco-2 cells that were left to develop in the incubator to be used in determining the ECT parameters became 60–70% confluent, they were removed with Trypsin-EDTA (Invitrogen), precipitated by centrifuging at 1000 rpm for 5 min. 10 μ L propidium iodide (PI) was added to 90 μ L of cell suspension at a density of 1×10^6 cell/mL and loaded into a 0.4 cm gap EP cuvettes (Bio-Rad, Hercules, CA, USA) that were used to determine cell electropermeabilization. Depending on the cell permeability, PI enters the cell and emits red fluorescent. To determine the cell mortality due to the electrical field, 400 μ L cell suspension with a density of 1×10^6 cell/mL was transferred to 0.4 cm EP cuvettes. All the cuvettes were placed individually in the EP device chamber (Bio-Rad, Hercules, CA, USA), and the electrical field application was made. The cells were subjected to 8 square wave pulses having electric field intensity ranging from 0 to 1250 V/cm with a frequency of 1 Hz and pulse duration of 100 μ s, which correspond to the parameters used in ECT clinical practice [18,29]. The cells that were used to determine the electropermeabilization were incubated with PI at room temperature for 15 min after the electrical field application. The electropermeabilization of the cells was measured with flow cytometry (Becton-Dickinson). To determine the cell mortality because of the electrical field, both short-term (20 min incubation) and long-term (24 h incubation) cell viability were examined. The short-term examination was carried out with the cell counting device, and the long-term examination was done with the MTT assay method.

2.4.3. Electrochemotherapy protocol

Caco-2 cells were cultured in the incubator at 37 °C, 90% humidity, and 5% CO₂ when the cells became 60–70% confluency, they were centrifuged at 1000 rpm for 5 min and resuspended at a density of 1×10^6 cells/mL in DMEM finally containing Co(II) or Ru(II) complexes at 200 μ M. 400 μ L of the cell suspension mixture was transferred to 0.4 cm EP cuvettes (Bio-Rad, Hercules, CA, USA) and subjected to the electric field. 8 square wave pulses having electric field intensity 1125 V/cm with a frequency of 1 Hz (duration of each electric pulse was 100 μ s) were applied to cell suspensions. The optimum EP parameters used in this study for the Caco-2 cell line were determined as a result of cell viability test and flow cytometry analysis after electroporation at different electrical fields (0–1250 V/cm). The cells that underwent only compound applications were also placed in EP cuvettes under the same conditions and times, but the voltage was not applied. Each experiment has been replicated four times. After electroporation application, 850 mL growth medium and 150 μ L suspension were added to each well of the 24 well cell culture plates and left for incubation. After 24 h of incubation, the efficiency of ECT was evaluated by analyzing cell viability with the MTT assay [30].

2.4.4. MTT assay

The cytotoxicity of the synthesized compounds was evaluated by using MTT (3-(4,5-dimethylthiazol-2-yl)-2,5-diphenyltetrazolium bromide) assay. The cells that underwent chemotherapy and ECT were seeded to the plates and left in the incubator containing 5% CO₂ and 95% humidity at 37 °C for 24 h. At the end of the incubation, the substance solutions in the wells were taken, 90 μ L DMEM and 10 μ L MTT solution were added to each well, and re-incubated in the incubator for another 4 h. After the 4 h incubation, the growth medium with MTT was removed from the medium, and 100 μ L DMSO was added to each well to dissolve the formazan crystals formed in the wells. The optical density (OD) of the color intensity forming in the wells was measured at 570 nm with Microplate Reader [31]. Only fresh medium was used as the control group. Since the MTT is affected by light, the experiments were conducted in a dark environment. The absorbance values obtained from the MTT assay of the groups in which the synthesized compounds were applied were proportioned to control absorbance value, and % viability value was calculated with the following formula.

% Viability

$$= \left(\frac{\text{Synthesis compound applied group OD}}{\text{Control group OD}} \right) \times 100$$

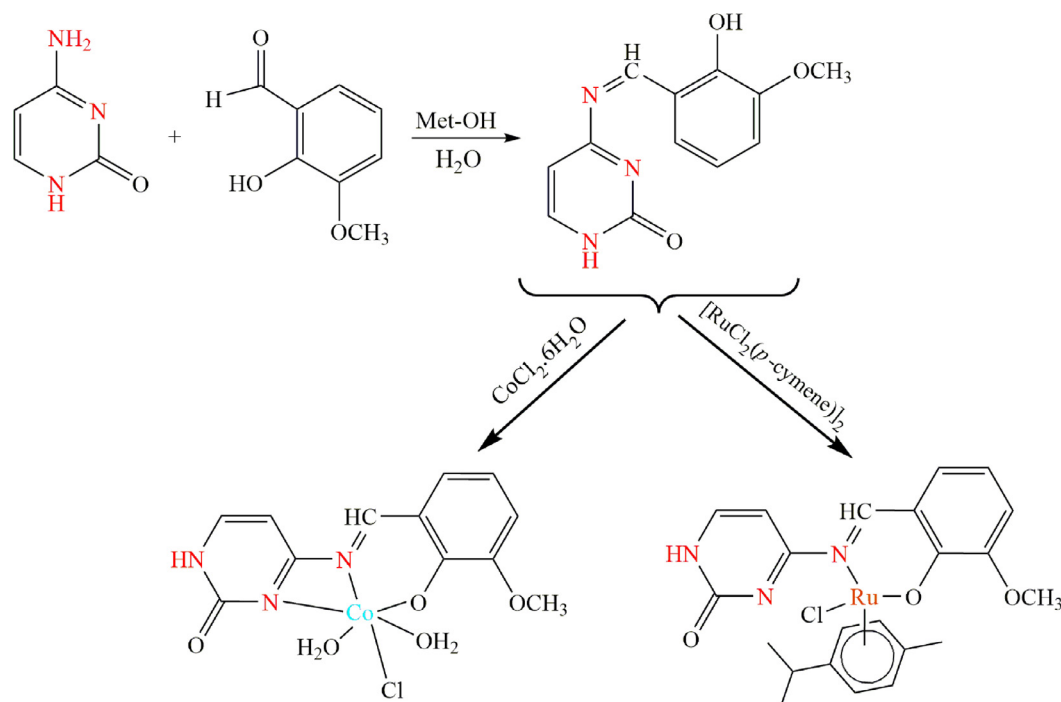
With the help of the graphic, the material concentration (IC₅₀), which provided 50% inhibition, was calculated by drawing inhibition percentage against material concentration. All analyses were studied as three parallels, and each parallel experiment contained repetitions between 6 and 8. The results are expressed as mean \pm standard deviation.

3. Result and discussion

3.1. Chemistry

All the compounds (Schiff base, cobalt and ruthenium metal complexes) found to be thermally stable at room temperature and soluble in methanol, ethanol and water. The solubility of these compounds in water is important for green chemistry and they are environmental friendly.

The FTIR spectrum of the Schiff base was compared with Co(II) and Ru(II) complexes in order to confirm the binding mode of the ligand. Schiff base important characteristic bands at around



Scheme 1. The proposed structures of Schiff base ligand and its Co(II), Ru(II) complexes.

3200, 1672, 1610, 1230 and 1107 cm^{-1} region which are ascribed to $\nu(\text{OH})$, $\nu(\text{C}=\text{N})$, $\nu(\text{C}=\text{N}$, pyrimidine ring), $\nu(\text{C}-\text{OCH}_3)$ and $\nu(\text{C}-\text{O})$, respectively. The $\nu(\text{CH}=\text{N})$ linkage band was altered towards lower wavenumber values by 14–19 cm^{-1} in the spectra of the metal complexes, confirming bonding of azomethine nitrogen to cobalt and ruthenium metal atom [24,32–35].

The FT-IR spectra of Co(II) and Ru(II) complexes were assigned through comparing the spectra Schiff base. The absence of the Schiff base ligand's phenolic hydroxyl (-OH) band in the region of 3358 cm^{-1} in the metal complexes confirming the coordination of phenolic group with the metal center in the complexes [36–38]. The formation of metal complexes was also proved through the emergence of new weak bands, Co(II) and Ru(II) complexes, non-ligand bands in the range of 587–523 cm^{-1} and 506–455 cm^{-1} . These new frequencies were attributed to the $\nu(\text{Co/Ru}-\text{O})$ and $\nu(\text{Co/Ru}-\text{N})$ vibrations respectively [36,39,40]. The significant bands of ligand and its Co(II) and Ru(II) complexes were given in experimental section.

Co(II) complex exhibited a strong absorption band in the region 3425, 857 cm^{-1} ascribed to $\nu(\text{OH})$ of water, which confirmed the presence of coordinated and a lattice water molecule. The event of water molecules in the structure of the complex was further confirmed by microanalysis and thermal analysis [41]. Single crystals for Co(II) and Ru(II) metal complexes could not be obtained from any solvent. The geometric structures of these complexes have been proposed based on analytical and spectral data. The proposed structures for Schiff base and Co(II), Ru(II) complexes are given in Scheme 1.

Electronic spectra of the Schiff base, Co(II) and Ru(II) complexes performed in the ethanol solution. The electronic spectrum exhibited high absorption bands in the 219–387 nm region may be attributed to the $\pi \rightarrow \pi^*$ and $n \rightarrow \pi^*$ transition of aromatic ring and azomethine group ($\text{C}=\text{N}$) groups/intramolecular charge transfer (CT) involving the whole molecule. The absorption band positions in the electronic spectrum of Co(II) complex was observed at broad absorption (614–648 nm) bands. These bands can be attributed to $\text{L} \rightarrow \text{M}$ charge-transfer [42–44]. The value of the magnetic moment of Co(II) complex recorded at 4.33 B.M., which is indicating for

octahedral geometry around the Co(II) ion [32,39,45]. The spectra of the Ru(II) complex showed intense bands in the range of 400–317 nm, which can be attributed to charge transfer from ligand to metal (MLCT) [36,37,42]. The electronic spectra of Ru(II) complex are reliable to the octahedral geometry.

The proton NMR spectra of the Schiff base ligand and Ru(II) complex mentioned in DMSO- d_6 . The phenolic OH signal of ligand was observed at 12.2 ppm. The singlet signal wasn't occurred on the spectra of Ru(II) complex. The disappearance of this signal confirmed the bonding of the phenolic oxygen atom with the metal ion by deprotonation [34,37,46–48].

Thermal analysis results of Schiff base ligand are given in Table 1 and mass analysis results are given in the experimental part.

3.2. Powder X-ray diffraction analyses

X-ray diffractometer (UltimaIV-Rigaku, $\text{CuK}\alpha=0.1540562$ nm) was used to test the structural properties of the complexes. Provided list showing working parameters of XRD; scanning mode: 2Theta/Theta, scanning type: continuous scanning, operating current: 30 mA, operating voltage: 40 Kv, scan step: 0.02°, scanning range: 10–90°. Fig. 1 provide XRD spectrums of Co(II) and Ru(II) complexes. Table 2 and Table 3 give crystal parameters (FWHM, grain size, diffraction angle detected) of the complexes.

3.2.1. XRD results of co(ii) complex

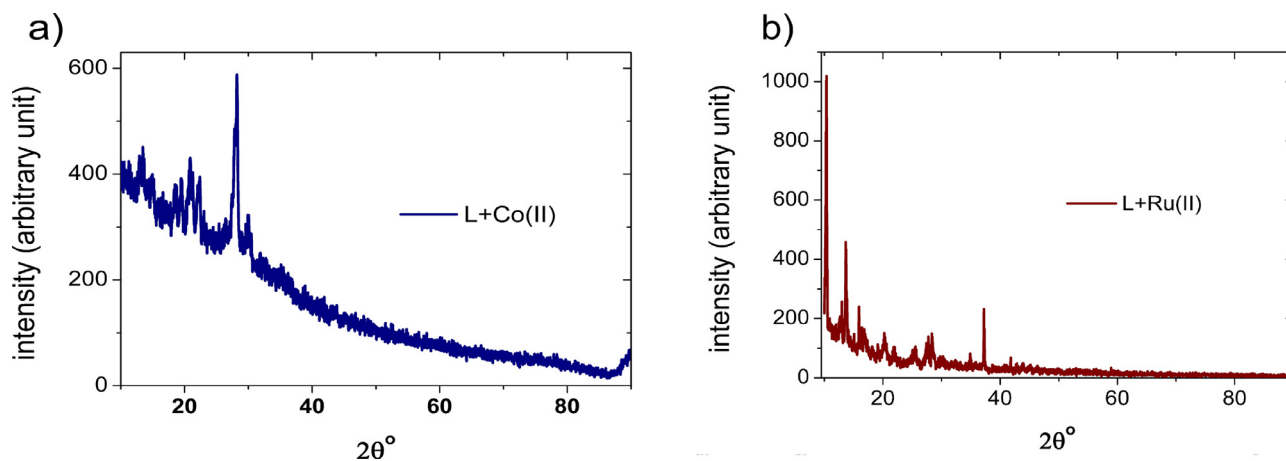
Fig. 1 shows the XRD phase behavior of the Co(II) complex. The peak (with high intensity, 590 (a.u)) at a 28.2° diffraction angle was observed. We produced the complex for the first time, so; is not available in the literature. But; Structural parameters of a similar complex were given in previous studies [47,49]. Using Scherer formula, grain sizes of the complex can be calculated;

$$R = \frac{g\lambda}{F\cos\theta} \quad (1)$$

λ shows X-ray wavelength, θ shows Bragg's diffraction angle, $g = 0.94$ shows constant, F shows full width of half maximum

Table 1
TGA data of Co(II) and Ru(II) complexes.

Complexes	Decomp. stages	The temperature range in TG (°C)	Wt. loss (mg)		Decomp. assignment
			Calcd. (Found)		
[CoCl·L(H ₂ O) ₂]-2H ₂ O	1	50–120	8.77	7.84	2H ₂ O
	2	120–220	8.77	8.96	2H ₂ O
	3	220–330	34.46	34.04	C ₇ H ₆ OCl
	4	330–850	29.72	29.53	C ₅ H ₄ ON ₃
Residue		>850	18.25	18.28	CoO
[RuCl(p-cymene)L]	1	240–285	15.81	16.12	C ₂ H ₆ OCl
	2	285–350	41.56	41.03	C ₁₃ H ₁₄ ON ₂
	3	350–700	23.01	23.40	C ₇ H ₄ ON
Residue		>700	19.62	19.62	Ru metal

**Fig. 1.** XRD phase of Co(II), Ru(II) complex.**Table 2**
Grain size value of the Co(II) complex.

Full Width Half Maximum (F) (°)	2θ (°)	Grain Size (R)(nm)
0.58	28.2	14.41

Table 3
Grain sizes of the Ru(II) complex.

2θ (°)	Full Width Half Maximum (F)(°)	Grain Size (R)(nm)
10.3	0.16	51.91
13.6	0.14	59.37
15.9	0.07	118.82
37.2	0.09	93.42

intensity. The average grain sizes (R) of the complex were calculated from the highest peak intensity. Grain size values of the Co(II) complex are given in Table 2. The grain size of the related peak of the complex was found to be 14.41 nm.

3.2.2. XRD results of ru(ii) complex

Fig. 1 shows the XRD phase behavior of the Ru(II) complex. Four distinct peaks (with high intensity) were observed from the measurement. These peaks are given in following; 10.3° (intensity 1023 (a.u)), 13.6° (intensity 461 (a.u)), 15.9° (intensity 243 (a.u)), 37.2° (intensity 235 (a.u)). The highest intensity was found at the peak of 10.3°, while the lowest intensity was found at the peak of 37.2°. The measurement proves that the complex has a polycrystalline phase. The orientation of the detected peaks cannot be given because the complex is synthesized for the first time and is not available in the literature. By formula 1, we calculated grain sizes of our complex, as shown in Table 3. We had the highest grain size to be 118.82 nm at 15.9° diffraction angle, the lowest grain size to be 51.91 nm at 10.3°.

Table 4
IC₅₀ values of the ligand and its Co(II) and Ru (II) complexes in Caco-2 and L-929 cells.

Compounds	Caco-2 IC ₅₀ (μM)	L-929 IC ₅₀ (μM)
L	803,65	964,46
Co(II) complex	609,6	1008,73
Ru(II) complex	510,26	1213,83

3.3. Anticancer activity

3.3.1. MTT assay results

Nine different concentrations of the synthesized ligand and its Co(II) and Ru(II) complexes (10; 25; 50; 100; 200; 300; 400; 500; 600 μM) were treated with the Caco-2 and L-929 cells for 24 h, and their absorbances were measured spectrophotometrically. The percent inhibition values of the Caco-2 and L-929 cells were calculated by the measured absorbances. The inhibition that occurred in cell proliferation was determined by the MTT assay. Whether the test agents had cytotoxic effects on colon cancer and mouse fibroblast cells was tried to be determined by calculating the IC₅₀ values (Table 4).

The cytotoxic effects of the chemical test agents applied in vitro to Caco-2 and L-929 cells were determined according to IC₅₀ values. Low IC₅₀ shows high cytotoxicity, and high IC₅₀ shows low cytotoxicity. According to IC₅₀ values, the Ru(II) complex of the ligand showed the best cytotoxic effect. This complex also had a very low cytotoxic effect on the L-929 normal cell line. The Co(II) complex had anticancer effects similar to the Ru(II) complex; however, was not as strong as it. The ligand, on the other hand, had the lowest anticancer activity with the highest IC₅₀ value in both cell lines. The Ru(II) complex at 10 μM to 400 μM concentration range, and the Co(II) complex at 10 μM - 300 μM concentration range did not produce significant cytotoxic effects in L-929 cells. Higher con-

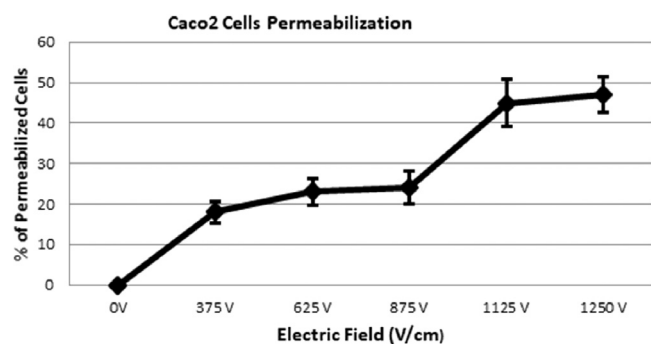


Fig. 2. Percentage of electropermeabilized Caco-2 cells 20 min after the treatment. The data is given as the mean \pm SD of three independent experiments.

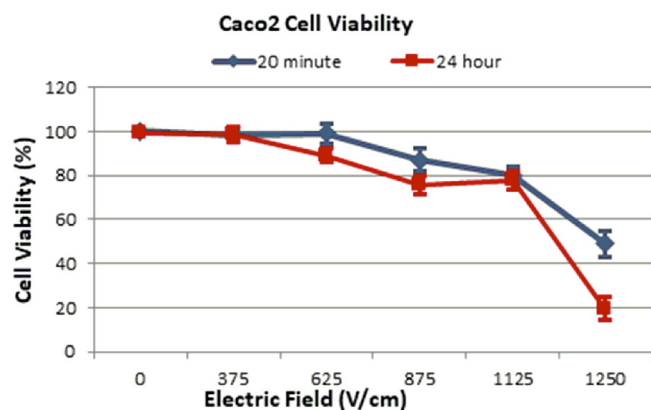


Fig. 3. Cell viability of Caco-2 cells at 20 min and 24 h after electroporation treatment. Data from four independent experiments are presented as mean \pm SD.

centrations began to affect L-929 normal cells. For this reason, ECT studies were continued with 200 μ M doses of Co(II) and Ru (II) complexes.

3.3.2. Optimal electric field parameters

The electropermeabilization of Caco-2 cells was determined by Flow Cytometry according to PI uptake. The permeability percentages of the Caco-2 cell membrane against different electrical fields (0–1250 V/cm) are given in Fig. 2.

With the increasing intensity of the electrical field pulses applied, there was a gradual increase in cell permeability. However, the permeability increased sharply at 875 V/cm and reached a 45% permeability rate at 1125 V/cm. No significant change was observed in the permeabilized cells after 1125 V/cm. The change in the cell viability rate (%) against different electric field applications was analyzed after 20 min and 24 h incubation, and the results are presented in Fig. 3.

The low electrical field applications up to 625 V/cm did not cause a significant decrease in cell viability. At 1125 V/cm, cell viability was approximately 77% in both short-term and long-term analysis results. As seen in Fig. 3, sharp decreases were observed in cell viability after 1125 V/cm. The optimum electroporation conditions of the Caco-2 cell line used in the study were determined as 1125 V/cm (1 Hz, 100 μ s and 8 pulses) as a result of the cell viability test and flow cytometry analysis. This value is ideal for ECT (compound + EP) treatment of Caco-2 cancer cells.

3.3.3. Cell viability due to electrochemotherapy

Complex-alone and complex+EP application groups' cell viability percentages after 24 h incubation were determined by the MTT assay, and the data are given in Fig. 4.

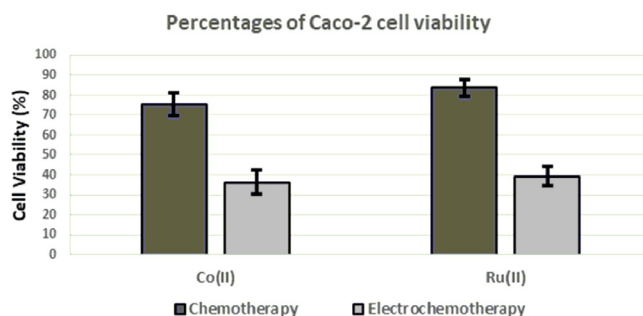


Fig. 4. Cell viability of Caco-2 cancer cells due to chemotherapy (complex-alone) and ECT (complex+EP) treatments after 24 h incubation. Data from four independent experiments are presented as mean \pm SD.

As seen in Fig. 4, the combined application of the complexes+EP (ECT) caused a significant decrease in Caco-2 cancer cell viability (%). There were great differences in terms of cell viability between complex (Co or Ru) alone and complex (Co or Ru)+EP groups. However, the resistance of the cell membrane against chemotherapy drugs and the drug resistance, which develops in cancer cells, causes that the treatment is prolonged, and the side effects are increased in patients by causing high-dose drug use [50]. Since ECT offers a short and effective treatment with very low drug doses of chemotherapeutic agents, it can minimize their negative side effects. The application of electrical impulses to the cells together with cytotoxic agents increases the permeability of the cell membrane and facilitating the transport of the agents into the cell [15]. The effectiveness of ECT depends on different parameters such as the type, number, duration, frequency and amplitude of the applied electrical pulses because these parameters can change the cell permeability and infrastructure [15,51]. For this reason, it is very important to determine appropriate electrical parameters before ECT. The optimum EP parameters used in this study for the Caco-2 cell line were determined as 1125 V/cm (1 Hz, 100 μ s duration and 8 pulses) as a result of cell viability test and flow cytometry analysis after electroporation at different electrical fields (0–1250 V/cm).

In the present study, Co(II) and Ru(II) complexes had similar cytotoxic effects in Caco-2 cells in both chemotherapy and ECT methods. However, their cytotoxicity increased dramatically in ECT treatment. It was observed that the application of Co(II) and Ru(II) complexes together with EP reduced cell viability to an average of 36.35%, and 39.27%, respectively. These results show that EP increases the cytotoxicity of Co(II) and Ru(II) complexes in Caco-2 cells. DNA is the most important target of anticancer agents in the cell [52]. The interaction of DNA with metal complexes may cause DNA fragmentation and cell death. ECT may have made it easier for the complexes to access Caco-2 cells, and damage the DNA by increasing intracellular concentrations.

It was shown that the electrical pulses applied in ECT also regulated the tumor blood flow. As a result of electrical pulses, the blood flow in tumors and partial oxygen pressure (pO₂) decreases [53], which, in turn, increases the effectiveness of anticancer drugs. Because anticancer drugs remain inactive in cells with abundant oxygen [54]. Many *in-vivo* and *in-vitro* studies conducted on different chemotherapeutic drugs showed the effectiveness of ECT [18,19,22,54,55]. Eşmekaya et al. [19] showed that the cisplatin + EP treatment is much more effective than cisplatin treatment alone. They suggested that cisplatin cytotoxicity increased in ECT, and that treatment could be provided with low-dose cisplatin in neuroblastoma treatment. Mittal et al. [56] reported that ECT enhances the effect of curcumin, and further studies were needed to increase the use of ECT with curcumin and various other drugs or vaccines in clinical practice. Although there are

many studies like these, no studies were examining the effect of ECT on ligand and metal complexes.

4. Conclusion

A new Schiff base and its two complexes $[\text{CoCl}(\text{H}_2\text{O})_2] \cdot 2\text{H}_2\text{O}$, $[\text{RuCl}(p\text{-cymene})\text{L}]$ were synthesized. Geometric structures of newly synthesized metal complexes were determined based on the results of FT-IR, UV-Vis., ^1H (proton), ^{13}C (carbon) NMR, CHN microanalysis, mass spectrum, magnetic susceptibility and thermal analysis. All spectroscopic data supports the formation of an octahedral structure to the Co(II) and Ru(II) metal complexes. In vitro anticancer activities of the newly synthesized compounds were evaluated on the human Caco-2 cancer cell line and biocompatibility characteristics were determined in the L-929 normal cell line by using the MTT assay. Furthermore, we examined the effectiveness of ECT on cytotoxic activities of these compounds in the Caco-2 cancer cell line. Co(II) and Ru(II) complexes showed considerable anticancer properties in Caco-2 colon cancer cells; however, the ligand did not show significant anticancer activity. In addition, these compounds demonstrated a low cytotoxic effect on L-929 normal cell line. It was determined that the combined application of EP+Complex was much more effective than the application of complexes alone in the treatment of Caco-2 colon cancer cells. These synthesized complexes can be developed as chemotherapeutic agents for colon cancer treatment and can yield promising results in combined applications with EP. Further studies are needed to expand the application of ECT with different complexes, drugs and vaccines.

Credit Author Statement

Kenan Buldurun and Nevin Turan performed the experiments, analyzed the data, XRD studies and wrote the manuscript. Mehmet Eşref Alkış, Ünzile Keleştemür and Yusuf Alan contributed to biological activity evaluation.

Declaration of Competing Interest

We declare that they have no known competing financial interests or personal relationships that could have appeared to affect the work reported in this article.

Acknowledgments

This work is supported by the Scientific Research Project Fund of Muş Alparslan University under the project number BAP-18-MMF-4901-02.

Supplementary materials

Supplementary material associated with this article can be found, in the online version, at [doi:10.1016/j.molstruc.2020.129402](https://doi.org/10.1016/j.molstruc.2020.129402).

References

- [1] J. Saranya, S.J. Kirubavathy, S. Chitra, A. Zarrouk, K. Kalpana, K. Lavanya, B. Ravikiran, Tetradentate Schiff base complexes of transition metals for antimicrobial activity, Arab. J. Sci. Eng 45 (2020) 4683–4695, doi:10.1007/S13369-020-04416-7.
- [2] E. Keskioglu, A.B. Gunduzalp, S. Cete, F. Hamurcu, B. Erk, Cr(III), Fe(III) and Co(III) complexes of tetradentate (ONNO) Schiff base ligands: synthesis, characterization, properties and biological activity, Spectrochim. Acta A 70 (2008) 634–640, doi:10.1016/j.saa.2007.08.011.
- [3] S. Toroglu, E. Ispir, Antifungal and antimicrobial activities of new Schiff base and its metal complexes, Asian J. Chem 21 (7) (2009) 5497.
- [4] K. Buldurun, N. Turan, E. Bursal, A. Mantarç, F. Turkan, P. Taslimi, İ. Gülçin, Synthesis, spectroscopic properties, crystal structures, antioxidant activities and enzyme inhibition determination of Co (II) and Fe (II) complexes of Schiff base, Res. Chem. Intermediat 46 (2019) 283–297, doi:10.1007/S11164-019-03949-3.
- [5] C. Shiju, D. Arish, S. Kumaresan, Novel water soluble Schiff base metal complexes: synthesis, characterization, antimicrobial-, DNA cleavage, and anticancer activity, J. Mol. Struct. 1221 (2020) 128770, doi:10.1016/j.molstruc.2020.128770.
- [6] D. Kumar, S.I. Khan, B.L. Tekwani, P. Ponnann, D.S. Rawat, 4-Aminoquinoline-pyrimidine hybrids: synthesis, antimalarial activity, heme binding and docking studies, Eur. J. Med. Chem. 89 (2015) 490–502, doi:10.1016/j.ejmech.2014.10.061.
- [7] M.T. Basha, R.M. Alghanmi, M.R. Shehata, L.H. Abdel-Rahman, Synthesis, structural characterization, DFT calculations, biological investigation, molecular docking and DNA binding of Co(II), Ni(II) and Cu(II) nanosized Schiff base complexes bearing pyrimidine moiety, J. Mol. Struct. 1183 (2019) 298–312, doi:10.1016/j.molstruc.2019.02.001.
- [8] D.S. Shankar, N. Ganji, S. Daravath, K. Venkateswarlu, S. Raj, Evaluation of DNA interaction, free radical scavenging and biologically active compounds of thermally stable *p*-tolylmethanamine Schiff bases and their binary Co(II) and Ni(II) complexes, Chem. Data Coll. 28 (2020) 100439, doi:10.1016/j.cdc.2020.100439.
- [9] N. Ganji, V.K. Chityala, P.K. Marri, R. Aveli, V. Narendrula, S. Daravath, DNA incision evaluation, binding investigation and biocidal screening of Cu(II), Ni(II) and Co(II) complexes with isoxazole Schiff bases, J. Photoch. Photobio. B. 175 (2017) 132–140, doi:10.1016/j.jphotobiol.2017.08.038.
- [10] J.M. Gichumbi, H.B. Friedrich, Half-sandwich complexes of platinum group metals (Ir, Rh, Ru and Os) and some recent biological and catalytic applications, J. Organomet. Chem. 866 (2018) 123–143, doi:10.1016/j.jorganchem.2018.04.021.
- [11] M.A. Malik, M.K. Raza, O.A. Dar, Amadudin, M. Abid, M.Y. Wani, A.S. Al-Bogami, A.A. Hashmi, Probing the antibacterial and anticancer potential of tryptamine based mixed ligand Schiff base ruthenium (III) complexes, Bioorg. Chem. 87 (2019) 773–782, doi:10.1016/j.bioorg.2019.03.080.
- [12] V. Brabec, J. Pracharova, J. Stepankova, P.J. Sadler, J. Kasparkova, Photo-induced DNA cleavage and cytotoxicity of a ruthenium (II) arene anticancer complex, J. Inorg. Biochem. 160 (2016) 149–155, doi:10.1016/j.jinorgbio.2015.12.029.
- [13] L. Demontoux, V. Derangère, T. Pilot, C. Thinselin, A. Chevriaux, F. Chalmin, F. Bouyer, F. Ghiringhelli, C. Rébé, Hypotonic stress enhances colon cancer cell death induced by platinum derivatives and immunologically improves antitumor efficacy of intraperitoneal chemotherapy, Int. J. Cancer. 145 (2019) 3101–3111, doi:10.1002/ijc.32590.
- [14] M.A. Arafath, F. Adam, M.R. Razali, L.E.A. Hassan, M.B.K. Ahamed, A.M.S. Majid, Synthesis, characterization and anticancer studies of Ni(II), Pd(II) and Pt(II) complexes with Schiff base derived from N-methylhydrazinecarbothioamide and 2-hydroxy-5-methoxy-3-nitrobenzaldehyde, J. Mol. Struct. 1130 (2017) 791–798, doi:10.1016/j.molstruc.2016.10.099.
- [15] J. Sączko, I. Kamińska, M. Kotulska, J. Bar, A. Choromańska, N. Rembiałkowska, K. Bieżuńska-Kusiak, J. Rossowska, D. Nowakowska, J. Kulbacka, Combination of therapy with 5-fluorouracil and cisplatin with electroporation in human ovarian carcinoma model in vitro, Biomed. Pharmacother. 68 (2014) 573–580, doi:10.1016/j.biopha.2014.05.005.
- [16] D.A. Casciato, M.C. Territo, Manual of Clinical Oncology, Lippincott Williams & Wilkins, 2009.
- [17] T. Kamal, S.B. Khan, S. Haider, Y.G. Alghamdi, A.M. Asiri, Thin layer chitosan-coated cellulose filter paper as substrate for immobilization of catalytic cobalt nanoparticles, Int J Biol. Macromol. 104 (2017) 56–62, doi:10.1016/j.jbiomac.2017.05.157.
- [18] L.G. Campana, D. Miklavčič, G. Bertino, R. Marconato, S. Valpione, I. Imarisio, M.V. Dieci, E. Granziera, M. Cemazar, M. Alaibac, Electrochemotherapy of superficial tumors—Current status: basic principles, operating procedures, shared indications, and emerging applications, Semin. Oncol. 46 (2019) 173–191, doi:10.1053/j.seminoncol.2019.04.002.
- [19] M.A. Esmekaya, H. Kayhan, M. Yagci, A. Coskun, A.G. Canseven, Effects of electroporation on tamoxifen delivery in estrogen receptor positive (ER+) human breast carcinoma cells, Cell Biochem. Biophys. 75 (2017) 103–109, doi:10.1007/S12013-016-0776-z.
- [20] M. Fiorentzis, A. Viestenz, U. Siebolts, B. Seitz, S.E. Coupland, J. Heinzelmann, The potential use of electrochemotherapy in the treatment of uveal melanoma: in vitro results in 3D tumor cultures and in vivo results in a chick embryo model, Cancers (Basel) 11 (2019) 1344, doi:10.3390/cancers11091344.
- [21] U. Probst, I. Fuhrmann, L. Beyer, P. Wiggermann, Electrochemotherapy as a new modality in interventional oncology: a review, Technol. Cancer Res. T. 17 (2018) 1533033818785329, doi:10.1177/1533033818785329.
- [22] G. Serša, M. Čemažar, D. Miklavčič, Z. Rudolf, Electrochemotherapy of tumours, Radiol. Oncol. 40 (3) (2006) 163–174.
- [23] N. Esmaili, M. Friebe, Electrochemotherapy: a review of current status, alternative IGP approaches, and future perspectives, J. Heal. Eng. (2019) 1–11, doi:10.1155/2019/2784516.
- [24] A. Fetoh, O.A. El-Gammal, G.M.A. El-Reash, Antioxidant and antitumor activities of Cr(III), Mn(II), Fe(III), Cd(II), Zn(II) and Hg(II) complexes containing a carbohydrazone ligand ending by 4-pyridyl ring, J. Mol. Struct. 1173 (2018) 100–110, doi:10.1016/j.molstruc.2018.06.087.
- [25] A. Aktaş, Ü. Keleştemür, Y. Gök, S. Balcıoğlu, B. Ateş, M. Aygün, 2-Morpholinoethyl-substituted N-heterocyclic carbene (NHC) precursors and their silver (I) NHC complexes: synthesis, crystal structure and in vitro anticancer properties, J. Iran. Chem. Soc. 15 (2018) 131–139, doi:10.1007/S13738-017-1216-8.
- [26] Y. Sarı, C. Gürses, D.B. Celepci, Ü. Keleştemür, A. Aktaş, Ş. Yüksel, B. Ateş, Y. Gök, 4-Vinylbenzyl and 2-morpholinoethyl substituted ruthenium (II) complexes: design, synthesis, and biological evaluation, J. Mol. Struct. 1202 (2020) 127355, doi:10.1016/j.molstruc.2019.127355.

- [27] A. Tan, S. Kizilkaya, U. Keleştemür, A. Akdemir, Y. Kara, The Synthesis, anticancer activity, structure-activity relationships and molecular modelling studies of novel isoindole-1, 3 (2H)-dione compounds containing different functional groups, *Anticancer Agent. Med. Chem.* 20 (2020) 1368–1378, doi:10.2174/1871520620666200410080648.
- [28] J. Gehl, Electroporation: theory and methods, perspectives for drug delivery, gene therapy and research, *Acta Physiologic. Scand.* 177 (2003) 437–447, doi:10.1046/j.1365-201X.2003.01093.x.
- [29] G. Sersa, M. Cemazar, M. Snoj, *Electrochemotherapy of tumours*, *Curr. Oncol.* 16 (2009) 34 PMID: PMC2669236.
- [30] P. Kumar, A. Nagarajan, P.D. Uchil, Analysis of cell viability by the MTT assay, *Cold Spring Harb Protoc* 2018 (6) (2018) pdb. prot095505, doi:10.1101/pdb.prot095505.
- [31] S.D. Mahajan, W.-C. Law, R. Aalinkeel, J. Reynolds, B.B. Nair, K.-T. Yong, I. Roy, P.N. Prasad, S.A. Schwartz, Nanoparticle-mediated targeted delivery of antiretrovirals to the brain, *Method. Enzymol.* 509 (2012) 41–60, doi:10.1016/b978-0-12-391858-1.00003-4.
- [32] G.A. El-Reash, O. El-Gammal, S. Ghazy, A. Radwan, Characterization and biological studies on Co(II), Ni(II) and Cu(II) complexes of carbohydrates ending by pyridyl ring, *Spectrochim. Acta A* 104 (2013) 26–34, doi:10.1016/j.SAA.2012.11.008.
- [33] M. Saif, H.F. El-Shafiy, M.M. Mashaly, M.F. Eid, A. Nabeel, R. Fouad, Synthesis, characterization, and antioxidant/cytotoxic activity of new chromone Schiff base nano-complexes of Zn(II), Cu(II), Ni(II) and Co(II), *J. Mol. Struct.* 1118 (2016) 75–82, doi:10.1016/j.molstruc.2016.03.060.
- [34] L.H. Abdel-Rahman, R.M. El-Khatib, L.A. Nassr, A.M. Abu-Dief, F.E.-D. Lashin, Design, characterization, teratogenicity testing, antibacterial, antifungal and DNA interaction of few high spin Fe(II) Schiff base amino acid complexes, *Spectrochim. Acta A* 111 (2013) 266–276, doi:10.1016/j.saa.2013.03.061.
- [35] M.R. Rodríguez, J. Del Plá, O.E. Piro, G.A. Echeverría, G. Espino, R. Pis-Diez, B.S. Parajón-Costa, A.C. González-Baró, Structure, tautomerism, spectroscopic and DFT study of o-vanillin derived Schiff bases containing thiophene ring, *J. Mol. Struct.* 1165 (2018) 381–390, doi:10.1016/j.MOLSTRUC.2018.03.120.
- [36] S. Sathiyaraj, K. Sampath, R.J. Butcher, C. Jayabalakrishnan, Synthesis, DNA binding, antioxidant and cytotoxic activities of ruthenium (II) complexes of a Schiff base ligand, *Transit. Met. Chem.* 38 (2013) 291–298, doi:10.1007/S11243-013-9690-z.
- [37] I.B. Amali, M.P. Kesavan, V. Vijayakumar, N.I. Gandhi, J. Rajesh, G. Rajagopal, Structural analysis, antimicrobial and cytotoxic studies on new metal (II) complexes containing N2O2 donor Schiff base ligand, *J. Mol. Struct.* 1183 (2019) 342–350, doi:10.1016/j.molstruc.2019.02.005.
- [38] K. Buldurun, N. Turan, A. Aras, A. Mantarçı, F. Turkan, E. Bursal, Spectroscopic and structural characterization, enzyme inhibitions, and antioxidant effects of new Ru(II) and Ni(II) complexes of Schiff base, *Chem. Biodiverse.* 16 (2019) e1900243, doi:10.1002/cbdv.201900243.
- [39] S.J. Kirubavathy, S. Chitra, Structural, theoretical investigations and biological evaluation of Cu(II), Ni(II) and Co(II) complexes of mercapto-pyrimidine Schiff bases, *J. Mol. Struct.* 1147 (2017) 797–809, doi:10.1016/j.molstruc.2017.07.019.
- [40] H.S. Çalık, E. İspir, Ş. Karabuga, M. Aslantas, Ruthenium (II) complexes of NO ligands: synthesis, characterization and application in transfer hydrogenation of carbonyl compounds, *J. Organomet. Chem.* 801 (2016) 122–129, doi:10.1016/j.jorganchem.2015.10.028.
- [41] V. Sumalatha, A. Rambabu, N. Vamsikrishna, N. Ganji, S. Daravath, Synthesis, characterization, DNA binding propensity, nuclease efficacy, antioxidant and antimicrobial activities of Cu(II), Co(II) and Ni(II) complexes derived from 4-(trifluoromethoxy) aniline Schiff bases, *Chem. Data Coll.* 20 (2019) 100213, doi:10.1016/j.cdc.2019.100213.
- [42] M.A. Ayoub, E.H. Abd-Elnasser, M.A. Ahmed, M.G. Rizk, Some new metal (II) complexes based on bis-Schiff base ligand derived from 2-acetylthiophene and 2, 6-diaminopyridine: syntheses, structural investigation, thermal, fluorescence and catalytic activity studies, *J. Mol. Struct.* 1163 (2018) 379–387, doi:10.1016/j.molstruc.2018.03.006.
- [43] A.A. Soliman, M.A. Amin, A.A. El-Sherif, C. Sahin, C. Varlikli, Synthesis, characterization and molecular modeling of new ruthenium (II) complexes with nitrogen and nitrogen/oxygen donor ligands, *Arab. J. Chem.* 10 (2017) 389–397, doi:10.1016/j.arabjc.2015.04.001.
- [44] G. Devagi, F. Dallemer, P. Kalaivani, R. Prabhakaran, Organometallic ruthenium (II) complexes containing NS donor Schiff bases: synthesis, structure, electrochemistry, DNA/BSA binding, DNA cleavage, radical scavenging and antibacterial activities, *J. Organomet. Chem.* 854 (2018) 1–14, doi:10.1016/j.jorganchem.2017.10.036.
- [45] N.M. Hosny, M.A. Hussien, F.M. Radwan, N. Nawar, Synthesis, spectral, thermal and optical properties of Schiff-base complexes derived from 2 (E)-2-((z)-4-hydroxypent-3-en-2-ylideneamino)-5-guanidinopentanoic acid and acetylacetone, *J. Mol. Struct.* 1143 (2017) 176–183, doi:10.1016/j.molstruc.2017.04.063.
- [46] H. Vinusha, S.P. Kollur, H. Revanasiddappa, R. Ramu, P.S. Shirahatti, M.N. Prasad, S. Chandrashekar, M. Begum, Preparation, spectral characterization and biological applications of Schiff base ligand and its transition metal complexes, *Results Chem* 1 (2019) 100012, doi:10.1016/j.rechem.2019.100012.
- [47] A.A. El-Sherif, T.M. Eldebs, Synthesis, spectral characterization, solution equilibria, in vitro antibacterial and cytotoxic activities of Cu(II), Ni(II), Mn(II), Co(II) and Zn(II) complexes with Schiff base derived from 5-bromosalicylaldehyde and 2-aminomethylthiophene, *Spectrochim. Acta A.* 79 (2011) 1803–1814, doi:10.1016/j.SAA.2011.05.062.
- [48] D. Pandiarajan, R. Ramesh, Ruthenium (II) half-sandwich complexes containing thioamides: synthesis, structures and catalytic transfer hydrogenation of ketones, *J. Organomet. Chem.* 723 (2013) 26–35, doi:10.1016/j.jorganchem.2012.10.003.
- [49] P. Nithya, R. Rajamanikandan, J. Simpson, M. Ilanchelian, S. Govindarajan, Solvent assisted synthesis, structural characterization and biological evaluation of cobalt (II) and nickel (II) complexes of Schiff bases generated from benzyl carbazate and cyclic ketones, *Polyhedron* 145 (2018) 200–217, doi:10.1016/j.POLY.2018.02.008.
- [50] A.-M. Gao, Z.-P. Ke, F. Shi, G.-C. Sun, H. Chen, Chrysin enhances sensitivity of BEL-7402/ADM cells to doxorubicin by suppressing PI3K/Akt/Nrf2 and ERK/Nrf2 pathway, *Chem. Biol. Interact.* 206 (2013) 100–108, doi:10.1016/j.cbi.2013.08.008.
- [51] M.A. Esmekaya, H. Kayhan, A. Coskun, A.G. Canseven, Effects of cisplatin electrochemotherapy on human neuroblastoma cells, *J. Membrane Biol* 249 (2016) 601–610, doi:10.1007/S00232-016-9891-4.
- [52] K. Saleem, W.A. Wani, A. Haque, M.N. Lone, M.-F. Hsieh, M.A. Jairajpuri, I. Ali, Synthesis, DNA binding, hemolysis assays and anticancer studies of copper (II), nickel (II) and iron (III) complexes of a pyrazoline-based ligand, *Future Med. Chem.* 5 (2013) 135–146, doi:10.4155/FMC.12.201.
- [53] G. Sersa, M. Krzic, M. Sentjurc, T. Ivanusa, K. Beravs, V. Kotnik, A. Coer, H. Swartz, M. Cemazar, Reduced blood flow and oxygenation in SA-1 tumours after electrochemotherapy with cisplatin, *Br. J. Cancer.* 87 (2002) 1047–1054, doi:10.1038/sj.bjc.6600606.
- [54] D.J. Chaplin, G. Sersa, *Application of Electric Pulses in SA-1 Tumours in Mice*, *Anticancer Res* 21 (2001) 1151–1156.
- [55] M. Cemazar, G. Sersa, Recent Advances in Electrochemotherapy, *Bioelectricity* 1 (2019) 204–213, doi:10.1089/BIOE.2019.0028.
- [56] L. Mittal, U.K. Aryal, I.G. Camarillo, V. Raman, R. Sundararajan, Effective electrochemotherapy with curcumin in MDA-MB-231-human, triple negative breast cancer cells: a global proteomics study, *Bioelectrochemistry* 131 (2020) 107350, doi:10.1016/j.bioelechem.2019.107350.